
Correlation of Lesional Uptake Parameters and Ratios with miPSMA Score and Estimating Normal Physiologic Concentration: An Exploratory Analysis in Metastatic Castration-Resistant Prostatic Carcinoma Patients with ^{68}Ga -PSMA-11 PET/CT

Ashwini Kalshetty^{1,2}, Biju Menon^{1,2}, Sutapa Rakshit^{1,2}, Atanu Bhattacharjee^{2,3}, and Sandip Basu^{1,2}

¹Radiation Medicine Centre, Bhabha Atomic Research Centre, Tata Memorial Centre Annexe, Mumbai, India; ²Homi Bhabha National Institute, Mumbai, India; and ³Department of Biostatistics, ACTREC, Tata Memorial Centre, Mumbai, India

The use of prostate-specific membrane antigen (PSMA)-based PET/CT has grown rapidly in recent years. This study estimated lesional uptake, normal physiologic concentrations, and temporal variation on delayed PET/CT of ^{68}Ga -PSMA-11 across different molecular imaging PSMA (miPSMA) expression scores in patients with metastatic castration-resistant prostatic carcinoma. **Methods:** We retrospectively studied 50 patients who were evaluated for ^{177}Lu -PSMA-targeted radioligand therapy and underwent ^{68}Ga -PSMA-11 PET/CT to determine disease status. Their mean age was 67.5 ± 8 y (52–84 y), and their average serum prostate-specific antigen level was $401 \pm 1,353$ ng/mL (0.098–9,235.13 ng/mL) at the time of scanning. They underwent standard ^{68}Ga -PSMA-11 PET/CT an average of 65 min after injection (60–90 min). Tumors ($n = 50$) were correlated with miPSMA expression score and uptake. Physiologic tracer distribution was estimated by placing a volume of interest 1 cm in diameter for smaller organs (submandibular, parotid, lacrimal, and tubarial glands; renal cortices; blood pool; and bowel) and 3 cm for larger organs (liver and spleen). SUV_{max} and SUV_{mean} were estimated for each region. Tumor-to-spleen (T/S), tumor-to-liver (T/L), and tumor-to-parotid (T/P) ratios were calculated for each lesion. For 16 patients who underwent a delayed scan an average of 135 min after injection (120–150 min), additional analysis evaluated the effect of the delay. **Results:** Uptake was maximal in renal cortices, followed by salivary glands, bowel, spleen, liver, lacrimal glands, and blood pool. SUV_{max} averaged 37.7 ± 22.1 for renal cortices, 15.4 ± 7.3 for submandibular glands, 14.4 ± 7.1 for parotid glands, 9.4 ± 4.9 for spleen, 6.2 ± 3.7 for lacrimal glands, 5.9 ± 2.3 for liver, 5.3 ± 1.41 for tubarial glands, 13.8 ± 7.6 for bowel, and 2.4 ± 1.9 for blood pool. SUV_{max} averaged 10.33 ± 3.27 (6.46–17) for miPSMA expression score 2 and 38.21 ± 25.9 (7.68–119.08) for score 3. T/S and T/P ratios averaged 1.21 ± 0.44 (0.48–2.04) and 0.6 ± 0.18 (0.39–0.87), respectively, for score 2 and 5.05 ± 4.46 (1.25–20.89) and 3.15 ± 2.09 (1.06–9.45), respectively, for score 3. SUV_{max} for score 3 lesions averaged 18.85, which increased significantly to 26.24 on delayed imaging ($P = 0.0001$). However, T/L, T/S, and T/P ratios did not significantly change. Temporal variation in normal organs showed SUV_{max} to increase significantly on delayed scans for

salivary (submandibular and parotid) and lacrimal glands and renal cortices, whereas SUV_{mean} increased significantly for spleen; liver; and parotid, tubarial, and lacrimal glands and insignificantly for other organs. **Conclusion:** These data form a basis for a proposed consensus on standard reference ranges for quantitative ^{68}Ga -PSMA-11 PET/CT. The temporal variations should be kept in mind for delayed acquisitions; T/S, T/L, and T/P ratios might serve as better markers for such scenarios.

Key Words: ^{68}Ga -PSMA-11 PET/CT; miPSMA score; ^{177}Lu -PSMA-617; metastatic castration-resistant prostate carcinoma; peptide receptor radioligand therapy; PSA

J Nucl Med Technol 2021; 49:235–240
DOI: 10.2967/jnmt.120.261289

Prostate-specific membrane antigen (PSMA)-labeled radioligands for PET/CT imaging in patients with prostate carcinoma have brought about a major change in the management of the disease. Furthermore, the recent introduction of PSMA-targeted radionuclide therapy for castration-resistant prostatic carcinoma patients has opened new areas of application for the theranostic pair for diagnosis and treatment, upholding the great promise of precision oncology. The role of PET/CT targeting of PSMA expression is well documented for staging and for detecting recurrence even in those with low serum prostate-specific antigen levels (1). Because of the high sensitivity and specificity of PSMA PET/CT, its use is currently expanding at various stages during the course of the disease.

The recently published PROMISE study has set guidelines for standard miTNM staging on PET/CT (2). Qualitative image assessment systems such as the molecular imaging PSMA (miPSMA) expression score are proposed as robust tools for defining objectivity in interpretation and staging (2,3), though they have yet to be validated for routine clinical use and their reproducibility in larger samples are yet to be tested. The miPSMA expression score takes into account the visual intensity of lesions relative to normal

Received Dec. 2, 2020; revision accepted Mar. 26, 2021.
For correspondence or reprints, contact Sandip Basu (drsamb@yahoo.com).
Published online July 9, 2021.
COPYRIGHT © 2021 by the Society of Nuclear Medicine and Molecular Imaging.

tracer uptake in internal reference organs such as the liver or parotid glands. Confirmation of normal biodistribution with the known range objectively can serve as an *in vivo* method of quality control as well as validate the observations made in the proposed scoring system, and there is a relative paucity of data on this topic, especially the temporal variation in such uptake (4–6). In this study, we attempted first to reproduce the reference ranges of ^{68}Ga -PSMA-11 in a subset of prostate carcinoma patients and subsequently to observe the correlation of miPSMA expression scores with various objective parameters such as SUV_{max} , tumor-to-spleen (T/S) ratio, tumor-to-liver (T/L) ratio, and tumor-to-parotid (T/P) ratio to supplement subjective observations and correlate semiquantitative values with miPSMA scores.

MATERIALS AND METHODS

In total, 50 patients with metastatic castration-resistant prostatic carcinoma who were being investigated for the feasibility of ^{177}Lu -PSMA-targeted radioligand therapy and underwent ^{68}Ga -PSMA-11 PET/CT either for staging or restaging in the past 2 y were retrospectively analyzed. The institutional medical ethics committee approved this retrospective study, and the requirement to obtain informed consent was waived. From the patient's medical records, we noted various general and clinical data such as patient age, Gleason score, history of surgery, history of prior therapy (hormonal therapy, chemotherapy, radiotherapy, or ^{177}Lu -PSMA-targeted radioligand therapy), and recent prostate-specific antigen levels. The mean age of the patients was 67.5 ± 8 y (range, 52–84 y), and the mean serum prostate-specific antigen level was $401 \pm 1,353$ ng/mL (range, 0.098–9,235.13 ng/mL) at the time of PET/CT scanning. The Gleason score was categorized as per the International Society of Urological Pathology Consensus grading, into 5 groups (7). The overall patient characteristics are described in Table 1.

PET/CT Acquisition Protocol

After appropriate preparation and quality control testing of the radiotracer, ^{68}Ga -PSMA-11, the patients were administered an average dose of 103.23 ± 22.2 MBq (range, 74–166.5 MBq) and 2 mL of furosemide (10 mg/mL) intravenously. After the injection, the patients were asked to drink an oral contrast medium (10 mL of sodium amidotrizoate and meglumine amidotrizoate [Urografin; Bayer]) diluted in 1 L of water within 1 h for optimal contrast in the abdominal pelvic region. The patients were asked to void before imaging to reduce urinary bladder activity, and whole-body scans were acquired at 65 min, on average (range, 60–80 min), after injection of the radiotracer. A subgroup of 16 patients underwent delayed scanning 135 min after injection, on average (120–150 min), after consenting to the procedure.

The PET/CT scans were acquired using a Philips Gemini TF 16 PET/CT scanner. A CT surview (90 kV, 20 mA) followed by a CT scan (100 mA; 120 kV; field of view, ~ 600 mm; CT slice thickness, 2.0 mm; standard resolution; collimation, 16×1.5 ; pitch, 0.813; matrix, 512×512) was performed for PET attenuation correction. After CT, whole-body PET was performed in 3-dimensional mode at 8–10 bed positions, with a 2-min emission per bed position, from the mid thighs to the base of the skull in the arms-up position.

TABLE 1
Patient Characteristics and Previous Therapies

Parameter	Data
Age (y)	
Mean \pm SD	67.5 \pm 8
Range	52–84
Serum prostate-specific antigen (ng/mL)	
Mean \pm SD	401 \pm 1,353
Range	0.098–9,235.13
Gleason score	
Group 1	1
Group 2	6
Group 3	9
Group 4	17
Group 5	17
Surgery (prostatectomy \pm orchidectomy) (n)	
Yes	50 (100%)
No	0 (0%)
Hormonal treatment (n)	
Yes	46 (92%)
No	4 (8%)
Chemotherapy (n)	
Yes	39 (78%)
No	11 (22%)
External-beam radiation therapy (n)	
Yes	24 (48%)
No	26 (52%)
^{177}Lu -PSMA therapy (n)	
Yes	16 (32%)
No	34 (68%)
Initial staging (n)	
Yes	11 (22%)
No	39 (78%)
Restaging (n)	
Yes	45 (90%)
No	5 (10%)

Images were reconstructed using a standard iterative algorithm based on the 3-dimensional row-action maximum-likelihood algorithm. The ^{68}Ga -PSMA PET/CT data were evaluated in a dedicated Philips EBW workstation.

Volume-of-Interest Measurements

The physiologic tracer biodistribution was assessed in each patient by placing spherical volumes of interest. These had a diameter of 1 cm for smaller organs (renal cortex, submandibular glands, parotid glands, lacrimal glands, the newly described tubarial glands (8), blood pool [abdominal and thoracic aorta], and bowel) and 3 cm for larger organs (liver and spleen). SUV_{max} and SUV_{mean} for each organ were estimated (average of 2 measurements for smaller organs and 3 for larger). The schematics of measurement are illustrated in Figure 1.

For the first part of the study, in which the miPSMA score was correlated with SUV, only the most intense lesion per patient was selected. In the second part, in which temporal analysis was performed on a smaller cohort, additional lesions per patient were considered to observe the trend in the delayed imaging. These lesions were considered in the following order: primary, nodes, bone (1 or 2), and then other soft-tissue metastases. All these lesions were closer in intensity to the index lesions measured in the first part.

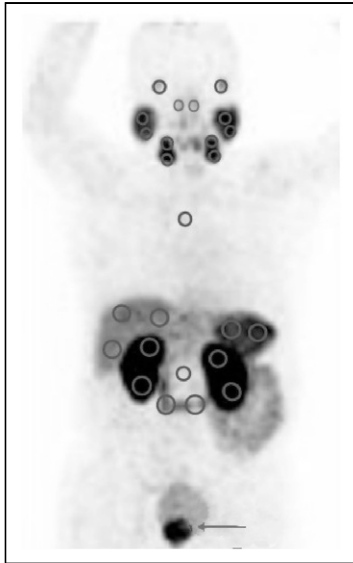


FIGURE 1. Schema for drawing volumes of interest adopted in this study. Arrow marks primary lesion in prostate.

SUV_{max} of these lesions, we also estimated T/P, T/S, and T/L ratios. For the subgroup of patients who underwent additional delayed imaging, the temporal variation in these parameters was analyzed.

Statistical Analysis

Continuous data were represented as mean with SD. All data were verified for normal distribution. Groups with equal variance were tested for any significant difference between them using a paired *t* test. The unpaired *t* test was used for groups with unequal variance. A *P* value of less than 0.05 was considered significant.

RESULTS

Physiologic Uptake

The SUV_{max} and SUV_{mean} of the organs with physiologic uptake are represented as average values with their SD, shown in Table 2. The renal cortices showed the highest SUV_{max} and SUV_{mean} , followed by salivary glands, bowel, spleen, lacrimal glands, liver, and blood pool. The mean SUV_{max} was 37.72 ± 22.1 for the renal cortices, $15.44 \pm$

In the subgroup of patients with additional delayed scans, we noted the same quantitative parameters in all regions in a similar manner. The lesions with maximum intensity in each scan was marked as the index lesion ($n = 50$). We used a fixed 1-cm volume of interest for measuring the SUV_{max} of such lesions. We measured additional lesions for the subgroup temporal analysis, amounting to total of 40 lesions. The miPSMA score was used for classifying the lesions as per the PROMISE trial (2).

We noted the SUV_{max} of all individual lesions against their grades. Apart from the directly measured

7.34 for the submandibular glands, 14.36 ± 7.05 for the parotid glands, 13.81 ± 7.6 for the bowel, 9.33 ± 4.98 for the spleen, 6.16 ± 3.68 for the lacrimal glands, 5.89 ± 2.32 for the liver, 5.3 ± 1.41 for the tubarial glands, and 2.36 ± 1.95 for the blood pool. A chart of the average SUV_{mean} and SUV_{max} for these regions is shown in Figure 2.

Tumor Lesions

When the lesions were classified as per the miPSMA expression score, we got primarily 2 categories, namely scores 2 and 3, as the patients at our center had been referred primarily to assess for ^{177}Lu -PSMA-targeted radioligand therapy feasibility and in that context had overt disease. The averages of SUV_{max} , T/S ratio, T/L ratio, and T/P ratio in each PSMA expression category were recorded. It appeared that score 3 lesions showed a mean of 3 times the PSMA expression of the parotid glands and 5 times than that of the spleen (Table 3). The presentation and the relative comparison of SUV_{max} , T/S ratio, T/L ratio, and T/P ratio for each category of lesions (scores 2 and 3) are illustrated in Figure 3. We performed unpaired *t* tests for these 2 scores of PSMA expression and found significant differences for all parameters (Table 3).

Temporal Variation in Uptake

The subgroup of 16 patients with paired early and delayed scan data also passed normality tests. Hence, paired *t* testing was performed.

Temporal Variation in Normal-Organ Physiologic Uptake

The paired *t* test assessed the variation in SUV_{mean} and SUV_{max} between the first and second scan groups. The average SUV_{mean} and SUV_{max} for most organs remained similar on delayed images. SUV_{max} was significantly increased in the salivary (submandibular and parotid) and lacrimal glands and in the renal cortices, whereas SUV_{mean} was significantly increased in the spleen and liver and in the parotid, tubarial, and lacrimal glands. The average SUV_{mean} and SUV_{max} in both studies, with their respective *P* values, are presented in Table 4.

Temporal Variation in Tumor Lesions

In total, 40 prominent lesions were identified in the subgroup of 16 patients who had dual-time-point imaging for evaluating the temporal variation in values. After applying paired *t* tests, we observed that SUV_{max} was significantly different from the baseline PET/CT scan (an increase on the delayed scan; $P = 0.0001$), whereas there was no significant difference in the T/S, T/L or T/P ratios. The results are in Table 5, and the temporal variation in the lesional parameters is plotted in Figure 4.

DISCUSSION

PSMA-based PET/CT imaging and theranostics have brought about a major change in the understanding and management of prostate cancer (9–17). The incorporation of semiquantitative and quantitative information continues to evolve and has the potential to enhance the fundamental

TABLE 2
 SUV_{mean} and SUV_{max} for Normal Organs

Organ	SUV_{mean}	SUV_{max}
Liver	3.98 ± 1.74	5.89 ± 2.32
Spleen	6.71 ± 3.8	9.33 ± 4.98
Kidneys	24.13 ± 15	37.72 ± 22.1
Submandibular glands	9.16 ± 4.56	15.44 ± 7.34
Parotid glands	9.51 ± 5.08	14.36 ± 7.05
Lacrimal glands	2.64 ± 1.46	6.16 ± 3.68
Blood pool	1.52 ± 1.22	2.36 ± 1.95
Bowel	7.7 ± 4.34	13.81 ± 7.6
Tubarial glands	2.7 ± 1.97	5.3 ± 1.41

Data are mean \pm SD.

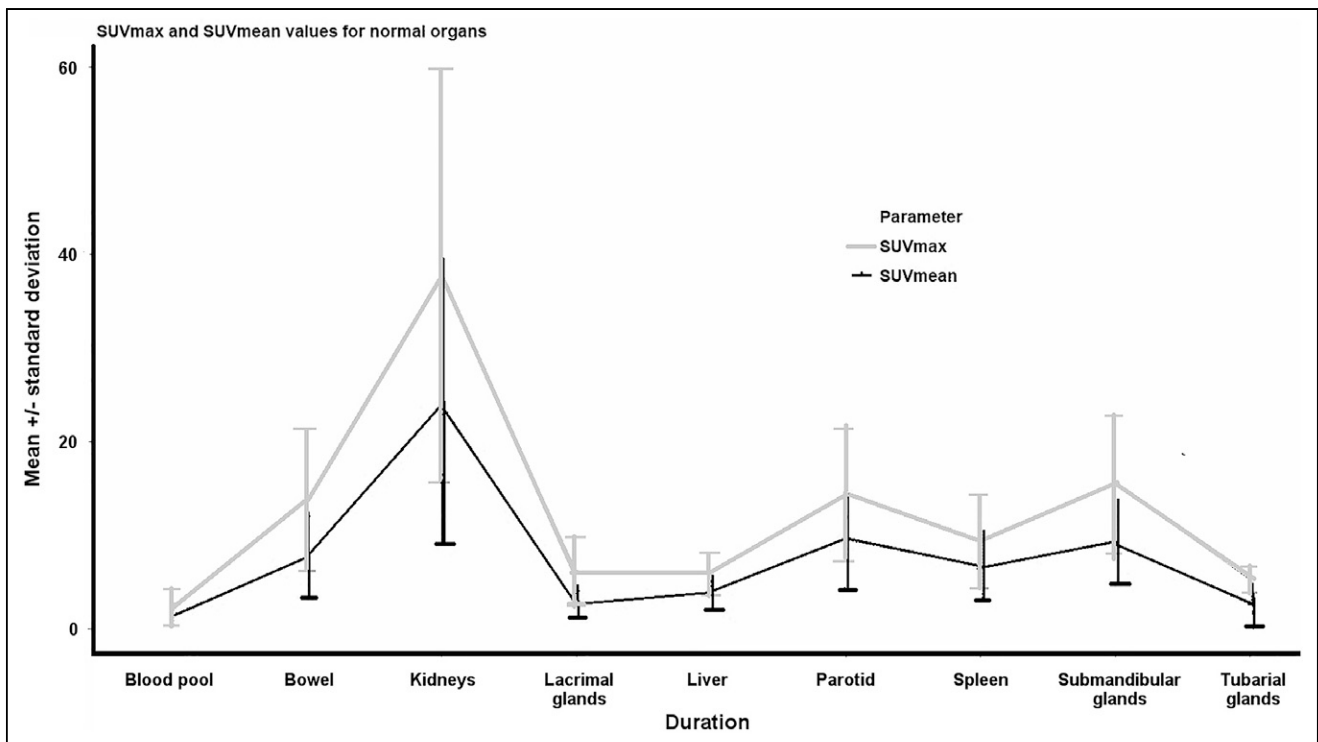


FIGURE 2. Average SUV_{max} and SUV_{mean} for different organs.

understanding of tumor heterogeneity, in vivo kinetics, and response to various therapies and hence can be a valuable supplement to visual interpretation and of paramount importance for undertaking clinical research (9,10,13,17). The present study analyzed ⁶⁸Ga-PSMA-11, the most common PET tracer used in prostate cancer diagnostics currently. Our results for the physiologic uptake align with some of the previously reported studies (4–6). Thus, we believe the present study results would allow a consistent pattern of reference range to be generated as a standard reference for future studies and research.

The miPSMA score as proposed by Eiber et al. (2) gives an elaborate description of miTNM staging on PSMA-based PET/CT. It is based on assigning a visual score from 0 to 3, with internal organs as reference points. When physiologic uptake is used as an internal reference for a scoring system, the ligand and biodistribution in the presence of high-volume disease have to be kept in mind and interpreted accordingly. The demonstration of SUV_{max} and its capacity to differentiate grades of lesions can elicit the incremental benefit of objective evidence to accurately assign the score.

Furthermore, to date, only a few studies have compared and addressed intra- and interpatient variability with ⁶⁸Ga- and ¹⁸F-labeled PSMA ligands, with the recommendation of using the spleen as the reference organ for ¹⁸F-PSMA-1007 (2,4–6). Besides these variations, other factors that also can influence uptake parameters, such as patient weight, injected dose, and wait duration, have not been conclusively studied. Hence, additionally, in the present study, we evaluated the effect of delayed imaging on SUV_{max} and SUV_{mean} in normal

organs, as well as SUV_{max}, T/S ratio, T/L ratio, and T/P ratio for tumor lesions.

In our study, the renal cortices showed the highest SUV_{max} and SUV_{mean}, followed by the salivary glands, bowel, spleen, lacrimal glands, liver, and blood pool. ⁶⁸Ga-PSMA-11 has been known to demonstrate high renal uptake, as stated in the literature, similar to the results obtained in our study (4–6). However, the maximum uptake in the kidneys was slightly higher in previous studies (4–6).

With respect to the temporal variation in normal physiologic uptake, SUV_{max} showed a significant increase on delayed scans in the salivary (submandibular and parotid) and lacrimal glands and in the renal cortices, whereas SUV_{mean} was significantly increased in the spleen and liver and in the parotid, tubarial, and lacrimal glands. In one

TABLE 3
Comparative Uptake Values and Ratios of Lesions

Parameter	Score of 2	Score of 3	P
Sample size (n)	11	39	
Average SUV _{max}	10.33 ± 3.27	38.2 ± 25.92	0.0009
SUV _{max} range	6.46–17.00	7.6–119.08	
Average T/S	1.21 ± 0.44	5.05 ± 4.46	0.0068
T/S range	0.48–2.04	1.25–20.89	
Average T/L	1.67 ± 0.46	6.98 ± 3.85	0.00004
T/L range	1.2–2.4	1.4–16.56	
Average T/P	0.61 ± 0.18	3.15 ± 2.09	0.00021
T/P range	0.39–0.87	1.06–9.45	

Data are mean ± SD or range.

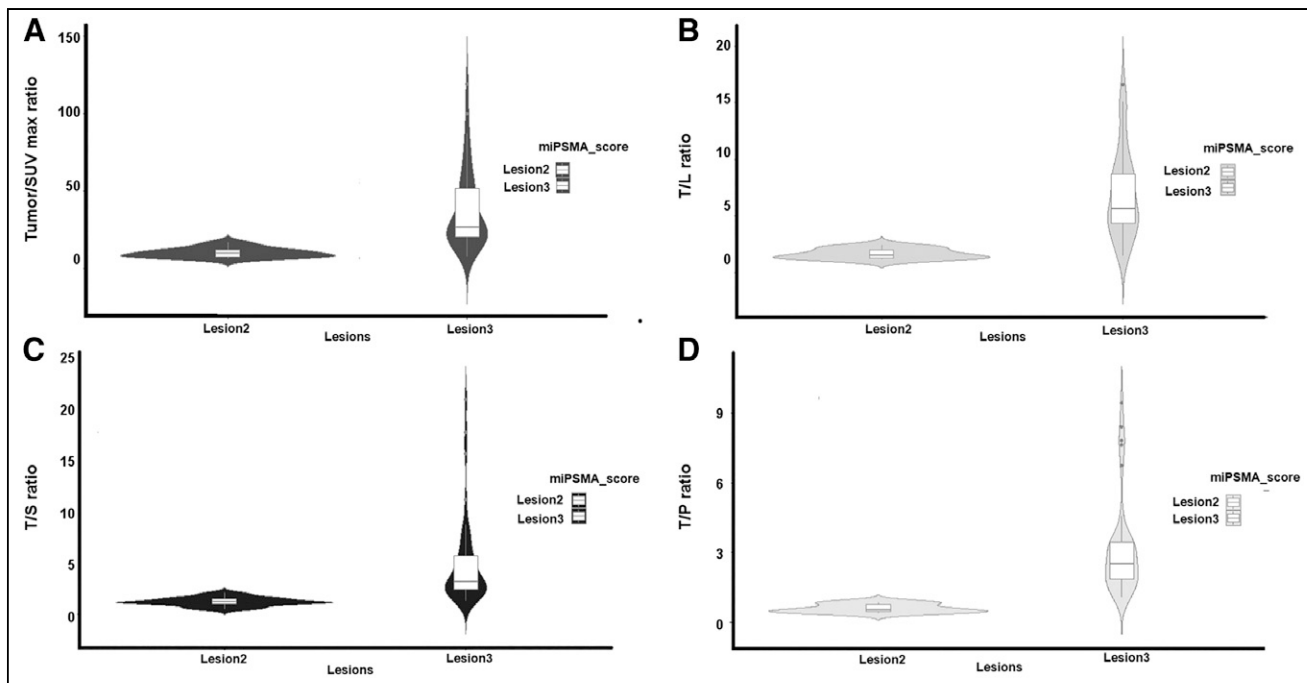


FIGURE 3. SUV_{max} , T/L ratio, T/S ratio, and T/P ratio for lesion 2 and lesion 3. Color version of this figure is available as supplemental file at <http://tech.snmjournals.org>.

TABLE 4
Comparative Temporal Variation of Mean SUV of Normal Organs with Their *P* Values

Organ	SUV_{mean}	SUV_{max}	SUV_{mean} delayed	SUV_{max} delayed	SUV_{mean} <i>P</i>	SUV_{max} <i>P</i>
Liver	3.6	5.9	3.1	6.7	0.0222	0.14
Spleen	6.5	9.4	5.8	9.1	0.0001	0.594
Kidneys	20.1	35.7	21.5	41.7	0.095	0.016
Submandibular glands	7.4	13.4	8.1	16.6	0.541	0.002
Parotid glands	7.1	12.9	8.5	14.1	0.047	0.037
Lacrimal glands	4.2	8.1	4.5	8.3	0.0267	0.01
Aorta	1.33	2.2	2.1	2.1	0.411	0.914
Bowel	5.5	9.7	5.4	10.9	0.41	0.44
Tubarial glands	2.87	5.55	3.3	6.06	0.02	0.08

previous study, no correlation was found between the uptake time and ^{68}Ga -PSMA-11 SUV_{peak} in the liver (4). The semi-quantitative measurements in our study have additionally demonstrated that the temporal variation in uptake is especially significant for lesions as well. Although the SUV_{max} of lesions as a standalone parameter varied significantly with time, the T/S and T/P ratios did not show a significant change. This observation would indicate that such temporal variations need to be kept in mind while interpreting images with delayed acquisitions and that T/S, T/L, or T/P ratio may be considered better parameters. The other area in which these values can have potential implications is treatment response assessment: the role of the quantitative parameters with receptor-based PET/CT continues to be in a development phase, and the various SUVs and ratios and their correlation with visual scoring can be useful for this purpose.

The limitations of this study are related to its retrospective nature, the limited number of cases, and its use of a

TABLE 5
Paired *t* Test Mean Values for Temporal Variation of Lesional Parameters Between Early and Delayed Images

Parameter	Early imaging	Delayed imaging	Paired <i>t</i> test <i>P</i>
SUV_{max}	18.85	26.24	0.0001
T/L ratio	5.9	6.65	0.45
T/S ratio	12.89	14.12	0.84
T/P ratio	9.36	9.05	0.62

single-center source. We did not study the effect of, or variations in, SUV normalized by lean body mass, which has been postulated to be a more robust parameter for quantitative analysis (18). Our study aimed to establish a reference range for normal organs; however, coexisting pathologies in reference organs, though rare in a given case scenario, are possible (e.g., splenic hemangioma). When present, they would need to be validated, and outliers can be

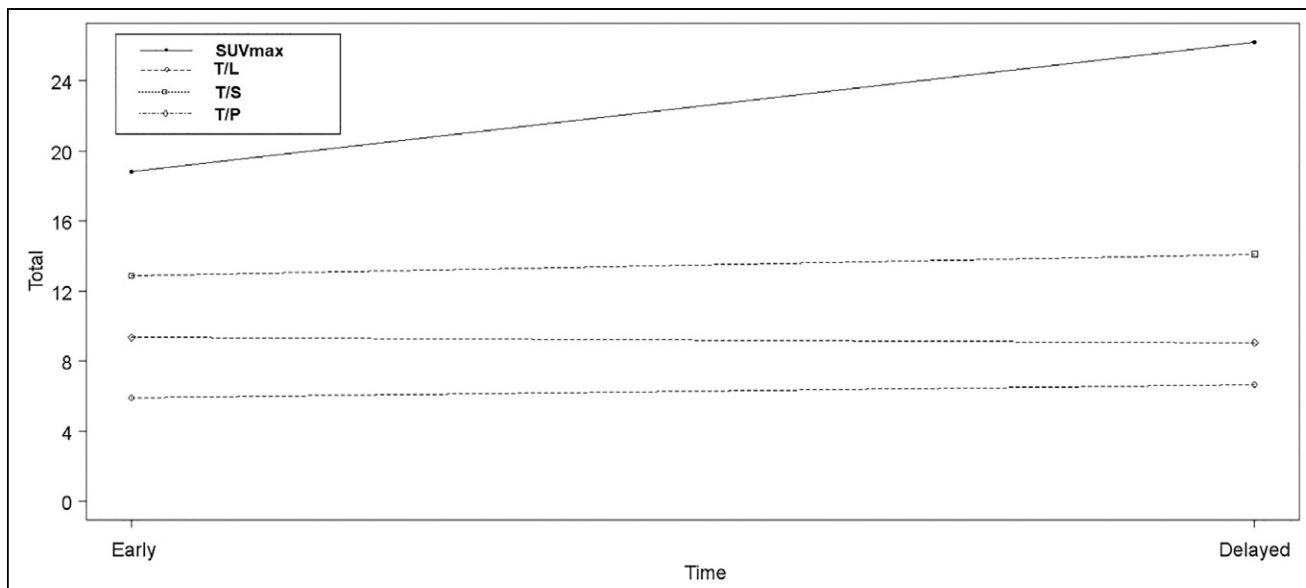


FIGURE 4. Comparison of SUV_{max} , T/L ratio, T/S ratio, and T/P ratio between scores 2 and 3.

identified. In the present study, the ratios were generated from a holistic perspective rather than a particular case in isolation. As standardization of such reference values becomes acceptable, we can get a general idea on distinguishing between normal and abnormal. We also have to mention that partial-volume effect was not considered in lesion selection in this analysis; the SUV and visual score of a very small lesion may be underestimated because of the partial-volume effect.

CONCLUSION

The reference ranges of normal organs (physiologic uptake) and tumor lesions for uptake and ratios for miPSMA scores of 2 and 3 were documented and established in the present study. On the basis of these data, a consensus on standard reference ranges can be generated for quantitative ^{68}Ga -PSMA-11 PET/CT. The temporal variation trends in lesions and reference organs should be kept in mind for delayed acquisitions. T/S, T/L, or T/P ratios serve as better markers for such scenarios.

DISCLOSURE

No potential conflict of interest relevant to this article was reported.

REFERENCES

- Fendler WP, Eiber M, Beheshti M, et al. ^{68}Ga -PSMA PET/CT: joint EANM and SNMMI procedure guideline for prostate cancer imaging—version 1.0. *Eur J Nucl Med Mol Imaging*. 2017;44:1014–1024.
- Eiber M, Herrmann K, Calais J, et al. Prostate cancer molecular imaging standardized evaluation (PROMISE): proposed miTNM classification for the interpretation of PSMA-ligand PET/CT. *J Nucl Med*. 2018;59:469–478.
- Rowe SP, Pienta KJ, Pomper MG, Gorin MA. PSMA-RADS version 1.0: a step towards standardizing the interpretation and reporting of PSMA-targeted PET imaging studies. *Eur Urol*. 2018;73:485–487.

- Ferreira G, Iravani A, Hofman MS, Hicks RJ. Intra-individual comparison of ^{68}Ga -PSMA-11 and ^{18}F -DCFPyL normal-organ biodistribution. *Cancer Imaging*. 2019;19:23.
- Prasad V, Steffen IG, Diederichs G, Makowski MR, Wust P, Brenner W. Biodistribution of [^{68}Ga]PSMA-HBED-CC in patients with prostate cancer: characterisation of uptake in normal organs and tumour lesions. *Mol Imaging Biol*. 2016;18:428–436.
- Demirci E, Sahin OE, Ocak M, Akovali B, Nematyazar J, Kabasakal L. Normal distribution pattern and physiological variants of ^{68}Ga -PSMA-11 PET/CT imaging. *Nucl Med Commun*. 2016;37:1169–1179.
- Epstein JI, Egevad L, Amin MB, Delahunt B, Srigley JR, Humphrey PA; Grading Committee. The 2014 International Society of Urological Pathology (ISUP) Consensus Conference on Gleason Grading of Prostatic Carcinoma: definition of grading patterns and proposal for a new grading system. *Am J Surg Pathol*. 2016;40:244–252.
- Valstar MH, de Bakker BS, Steenbakkers RJHM, et al. The tubarial salivary glands: a potential new organ at risk for radiotherapy. *Radiother Oncol*. 2021;154:292–298.
- Demirci E, Kabasakal L, Şahin OE, et al. Can SUVmax values of ^{68}Ga -PSMA PET/CT scan predict the clinically significant prostate cancer? *Nucl Med Commun*. 2019;40:86–91.
- Brito AET, Mourato FA, de Oliveira RPM, Leal ALG, Filho PJA, de Filho JLL. Evaluation of whole-body tumor burden with ^{68}Ga -PSMA PET/CT in the biochemical recurrence of prostate cancer. *Ann Nucl Med*. 2019;33:344–350.
- Miksch J, Bottke D, Krohn T, et al. Interobserver variability, detection rate, and lesion patterns of ^{68}Ga -PSMA-11-PET/CT in early-stage biochemical recurrence of prostate cancer after radical prostatectomy. *Eur J Nucl Med Mol Imaging*. 2020;47:2339–2347.
- Stone L. Predicting ^{68}Ga -PSMA-PET-CT positivity for recurrent disease. *Nat Rev Urol*. 2018;15:137.
- Verburg FA, Pfister D, Drude NI, Mottaghy FM, Behrendt FF. PSA levels, PSA doubling time, Gleason score and prior therapy cannot predict measured uptake of [^{68}Ga]PSMA-HBED-CC lesion uptake in recurrent/metastatic prostate cancer. *Nuklearmedizin*. 2017;56:225–232.
- Cem O, Torun N, Guler OC, Reyhan M, Yildirim BA, Yapar AF. Is there a correlation between Gleason score and maximum standardized uptake value in locally advanced prostate cancer patients? [abstract]. *J Clin Oncol* 2019 37(suppl):68.
- van Leeuwen PJ, Donswijk M, Nandurkar R, et al. Gallium-68-prostate-specific membrane antigen (^{68}Ga -PSMA) positron emission tomography (PET)/computed tomography (CT) predicts complete biochemical response from radical prostatectomy and lymph node dissection in intermediate- and high-risk prostate cancer. *BJU Int*. 2019;124:62–68.
- Jansen BHE, Kramer GM, Cysouw MCF, et al. Healthy tissue uptake of ^{68}Ga -prostate-specific membrane antigen, ^{18}F -DCFPyL, ^{18}F -fluoromethylcholine, and ^{18}F -dihydrotestosterone. *J Nucl Med*. 2019;60:1111–1117.
- Onal C, Guler OC, Torun N, Reyhan M, Yapar AF. The effect of androgen deprivation therapy on ^{68}Ga -PSMA tracer uptake in non-metastatic prostate cancer patients. *Eur J Nucl Med Mol Imaging*. 2020;47:632–641.
- Gafita A, Calais J, Franz C, et al. Evaluation of SUV normalized by lean body mass (SUL) in ^{68}Ga -PSMA11 PET/CT: a bi-centric analysis. *EJNMMI Res*. 2019;9:103.